Part III
Heat/Mass Transfer

9
Heat Transfer in Homogeneous Systems*

Franz Trachsel and Philipp Rudolf von Rohr

9.1
Introduction

Heat transfer in microchannels plays an important role in microreactor systems in terms of heating the reacting fluids or the dissipation of the heat of reaction. This chapter discusses heat transfer from the wall to the fluid in microchannels with diameters $d_h \leq 1$ mm. In laminar flow, the heat transfer coefficient is inversely proportional to the channel width, which makes microchannels favorable for high-performance heat exchange systems. Standard compact heat exchangers reach a surface-to-volume ratio larger than $800\,m^2\,m^{-3}$ with a typical feature size of less than 5 mm ($A/V = 4/d$). Micro heat exchangers have specific surface areas in the order of $10\,000\,m^2\,m^{-3}$ ($d = 400\,\mu m$). Tuckerman and Pease [1] reported efficient heat removal in a water-cooled silicon substrate up to a power density of $7900\,kW\,m^{-2}$ by downscaling the channel dimensions of the heat sink in the range of $50\,\mu m$. The increased surface-to-volume ratio makes microscale devices more appropriate for efficient heat transfer compared with conventional devices.

The fundamental mechanism behind heat exchange in microchannels does not differ from the well-established equations in macroscale applications. However, effects which are negligible and assumptions made in larger systems have to be re-evaluated and carefully considered on a smaller scale. A main concern with heat transfer in microchannel centers on the question of whether the conventional assumptions and theory can be applied.

This chapter gives an overview of recent literature concerning homogeneous heat transfer in microchannels ($d_h \leq 1$ mm). The influences of different effects on heat transfer which are more pronounced in microchannels compared with macroscale systems are discussed. Criteria are given when these different effects have to be considered. Conventional approaches to solve heat transfer problems in macroscale

*A List of Symbols and Abbreviations can be found at the end of this chapter.

Micro Process Engineering, Vol.1: Fundamentals, Operations and Catalysts
Edited by V. Hessel, A. Renken, J.C. Schouten, and J.-I. Yoshida
Copyright © 2009 WILEY-VCH Verlag GmbH & Co. KGaA, Weinheim
ISBN: 978-3-527-31550-5

applications are briefly summarized and their applicability to the microscale is discussed.

In the current literature on heat transfer in microchannels in homogeneous systems, large deviations between the different correlations and measurements can be seen. So far, no general conclusion can be drawn and the available heat transfer coefficient correlations are often restricted to the experimental setup and device used in a particular study. Therefore, there is still a need for precise experimental and numerical work in heat transfer analysis in microchannels to gain a better understanding.

Generally, it can be stated that as long as the continuum assumption holds, the classical heat transfer theory can be applied in microchannels assuming a linear relationship between heat flux and temperature and no jump of temperature at the fluid–solid boundary. The reason for the large discrepancies on comparing standard macroscale heat transfer correlations with microscale results is in the pronunciation of fluid effects and thermal effects which cannot be neglected at small scales. The influence of these effects on microscale heat transfer is multifaceted and many aspects contribute to a total analysis of such systems. In this chapter, we focus on the most important reasons for deviations of microchannel heat transfer from classical theory, such as axial heat conduction, surface roughness, viscous dissipation, thermophysical property variation, electric double layer and entrance region effects. Especially the experimental techniques and the accuracy of evaluated data have to be considered in the interpretation of microscale heat transfer measurements. The criteria included in this chapter support the reader's decision regarding how to adapt the assumptions and boundary conditions of standard heat transfer theory for specific microchannel geometries, fluids and flow situations. It is further recommended to conduct numerical simulations and experimental validation of the specific microreactor device for an optimized heat transfer within the microchannel. For characteristic channel dimensions of >1 mm, the conventional correlation summarized in Section 9.5 can be used, considering the assumed boundary conditions.

This chapter focuses on single-phase flow heat transfer in microchannels. For heat transfer of boiling and condensation in microchannels, the interested reader is referred to reviews by Kandlikar [2] and Thomé [3].

9.2 Continuum Assumption

The continuum model assumes continuous and indefinitely divisible matter. For gases the continuum model is valid when the mean free pathlength of the molecules λ is much smaller than the characteristic length of the flow L. The mean free path, depending on pressure and temperature of a gas molecule modeled as a rigid sphere, is

$$\lambda = \frac{1}{\sqrt{2}\pi n \sigma} = \frac{kT}{\sqrt{2}\pi p \sigma^2} \tag{9.1}$$

where n is the number of molecules per unit volume, σ the molecule diameter and k the Boltzmann constant.

The Knudsen number, Kn, defines the ratio between the mean free path and the characteristic length:

$$Kn = \frac{\lambda}{L} \tag{9.2}$$

In the continuum model ($Kn < 0.001$), the following assumptions can be made: (1) a linear relation between stress and strain, (2) no-slip boundary condition at the fluid–solid interface, (3) linear relation between heat flux and temperature and (4) no-jump condition of temperature at the fluid–solid interface. If the mean free path is not much smaller than the characteristic length, the flow is not near equilibrium and the above assumptions are no longer valid.

Continuum models (i.e. Navier–Stokes equation) should be used as long as possible in the applicable range. The mathematical handling is easier compared with molecular models, which have to be used in the non-continuum region.

9.2.1 Gases

In general, the continuum assumption is valid when $Kn < 0.001$. Empirically different Knudsen regimes have been determined, as shown in Figure 9.1.

Figure 9.2 shows the effective limits for approximations made for air with an "average air" molecule diameter of $\sigma = 4.15 \times 10^{-10}$ m. The mean molecular spacing under standard conditions is $\delta_0 = 3.3 \times 10^{-9}$ m. The mean molecular spacing is defined as

$$\delta \sim \left(\frac{\bar{V}_1}{N_A}\right)^{1/3} \tag{9.3}$$

where $\bar{V}_1$ is the molar volume and N_A is Avogadro's number.

9.2.2 Liquids

Since for liquids the concept of mean free path is not very useful, there is no accurate information on the conditions under which the basic assumptions for continuous

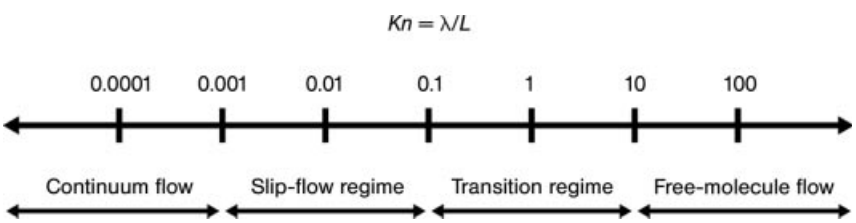

Figure 9.1 Knudsen number regimes. After Gad-el-Hak [4].

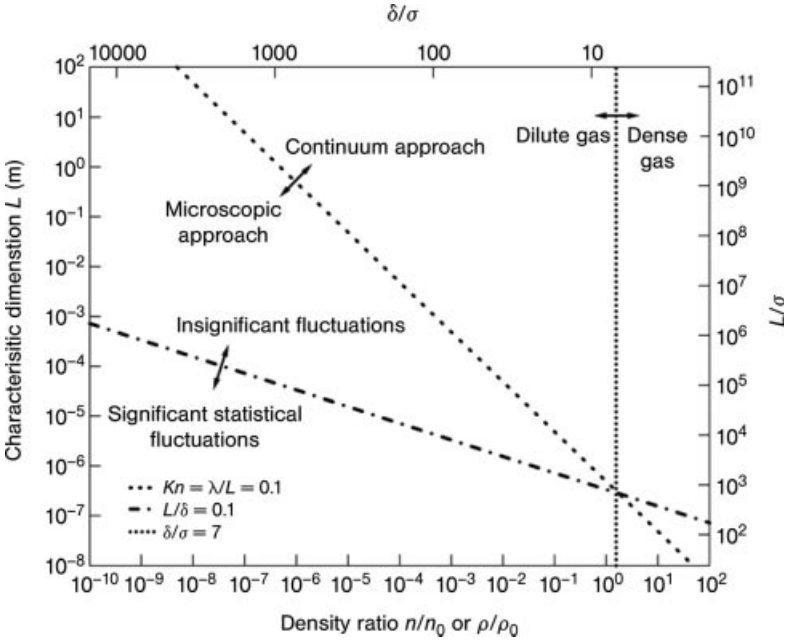

Figure 9.2 Limits of different approximations. Adapted from [5].

matter fail. The situation is more complex than in gases and experimental data show conflicting results. However, in general the incompressible Navier–Stokes equations describe the liquid flow in most microfluidic applications. An approximation of the beginning of non-Newtonian fluid behavior is given when the shear rate $\dot{\gamma}$ exceeds twice the molecular frequency scale [4]:

$$\dot{\gamma} = \frac{\partial u}{\partial y} \geq 2\tau^{-1} \tag{9.4}$$

with

$$\tau = \left(\frac{m\sigma^2}{\varepsilon}\right)^{1/2} \tag{9.5}$$

where τ is the molecular time scale, m the molecular mass, σ the molecular length scale and ε the molecular energy scale. For common fluids, the time scale in Equation (9.5) is extremely small; for water under standard conditions it is $\tau = 8.31 \times 10^{-13}$ s. This results in high shear rates at which the continuum approach would fail. Therefore, in small devices at extremely high speed or for a polymer with high molecular weight, non-Newtonian behavior of the liquid has to be considered.

Kleinstreuer [6] discusses alternative Knudsen numbers for liquid and gas–liquid systems, where the mean free path is replaced by the intermolecular length. The continuum approach then is valid for $Kn < 0.1$. For water under standard conditions, the Navier–Stokes equation holds in microchannels down to a feature size of 0.1 μm.

The global Kn for liquids is defined as

$$Kn = \frac{\lambda_{IM}}{L} \tag{9.6}$$

where λ_{IM} is the intermolecular length of the molecules (for water $\lambda_{IM} = 3$ Å) and L the characteristic length of the microfluidic system.

9.3 Heat Transfer in Homogeneous Microfluidic Systems

There is a large amount of literature concerning heat transfer in homogeneous microfluidic systems, with several recent reviews [7–12].

Figure 9.3 shows a summary of Nusselt number (Nu) correlations against Reynolds number (Re) in microchannels with $d_h \leq 1$ mm available from the literature up to the present date. The correlations are derived from either experiments and numerical or analytical considerations; however, for comparison, standard correlations for macro-scale tubes are additionally shown: the Hausen correlation [Equation (9.33)] for the laminar regime, the Gnielinski correlation [Equation (9.41)] for the transition region and the Dittus–Boelter correlation [Equation (9.39)] for the turbulent regime. To reach a sufficient residence time in chemical reactions, in most microreactor applications the small scale of the channels implies a laminar flow regime. As there is little agreement about the transition point from laminar to turbulent flow in microchannels, both laminar and turbulent correlations are included in the same graph.

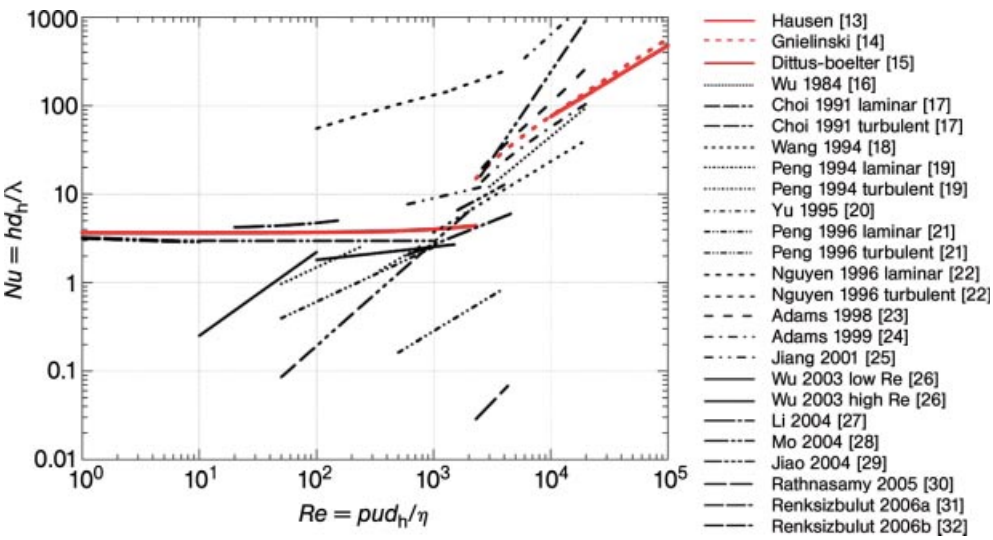

Figure 9.3 *Nu* number predictions from the literature for microchannels and macrochannels. The Reynolds number range covers laminar and turbulent flows.

In general, *Nu* increases with *Re*. A steeper increase of *Nu* with *Re* is observed in microchannel correlations, indicating a stronger dependence on *Re*. However, it is seen that little agreement exists between the different reports. In the low *Re* region, only sparse literature exists, since maximum heat transfer for heat exchangers is usually the goal of most studies. At higher *Re*, the different microchannel correlations both under- and overpredict the standard theory. In the laminar regime a *Re* dependence is seen and the Nusselt numbers are generally smaller than conventional ones. High Nusselt numbers with maximum deviations from conventional correlations were reported by Yu *et al.* [20] and Nguyen *et al.* [22]. Yu *et al.* [20] experimentally determined heat transfer coefficients of nitrogen and water flow in silica microtubes. The higher *Nu* values are explained by the eddy bursting phenomenon from the laminar sublayer in the turbulent core. Nguyen *et al.* [22] approximated the experimental data of water in trapezoidal Si–glass microchannels by a function dependent only on *Re*.

Higher heat transfer rates in turbulent microchannels than predicted by traditional large-scale correlations were observed by Adams *et al.* [23]. Based on the work of Gnielinski, a generalized correlation for turbulent single-phase flow in microchannels is derived:

$$Nu = Nu_{\mathrm{Gn}}(1+F) \tag{9.7}$$

where F is given by

$$F = CRe\left[1-\left(\frac{d}{D_0}\right)^2\right] \tag{9.8}$$

From the fitting of experimental data, the coefficients were calculated to be $C = 7.6 \times 10^{-5}$ and $D_0 = 1.164$ mm. This indicates that an enhancement of the heat transfer rate can be achieved with diameters smaller than 1.164 mm. The range of validity is $2.6 \times 10^3 \leq Re \leq 2.3 \times 10^4$, $1.53 \leq Pr \leq 6.43$ and $0.012\ \mathrm{mm} \leq d \leq 1.09\ \mathrm{mm}$.

In contrast, low Nusselt numbers were described by Choi *et al.* [17], Peng and Peterson [21], Wu and Cheng [26] and Rathnasamy *et al.* [30]. Choi *et al.* [17] suggested the suppression of eddy motion in the radial direction for small *Nu* and a dependence on *Re*. Peng and Peterson [21] examined heat transfer in parallel microchannels. They stated that geometric parameters such as the center-to-center distance of parallel microchannels have a significant influence on heat transfer. Wu and Cheng [26] also concluded that channel geometry has a great effect on *Nu*. Rathnasamy *et al.* [30] suggested a strong role of internal fluid thermal resistance and conjugated heat transfer effects on *Nu*.

Ameel *et al.* [33] studied hydrodynamically fully developed laminar flow in circular channels when slip flow occurs. An *Nu* correlation in the slip flow regime was derived:

$$Nu = \frac{48(2\beta-1)^2}{(24\beta^2-16\beta+3)\left[1+\frac{24\kappa(\beta-1)(2\beta-1)^2}{(24\beta^2-16\beta+3)(\kappa+1)Pr}\right]} \tag{9.9}$$

where $\beta = 1 + 4Kn$ and κ is the ratio of the specific heats. It was seen that Nu decreases with increasing Kn. At $Kn = 0$, the expression gives the well-known value of $Nu = 4.3636$. The thermal entry length could be described as

$$l_{th} = 0.0828 + 0.14Kn^{0.69} \tag{9.10}$$

Figure 9.3 clearly shows that different applications measure different heat transfer coefficients and no general correlation for single-phase heat transfer in microchannels can be derived so far.

The complete expressions of the Nu correlations in Figure 9.3 are shown in Table 9.1. Additionally, the experimental or numerical conditions are listed.

9.4 Pronounced Effects in Microchannel Heat Transfer

The heat transfer in microchannels is expected to agree with conventional theory provided that the discussed continuum assumptions can be made. For example, under fully developed laminar flow conditions at low Re, Nu is constant. However, many experimental data show large deviations between each other and inconsistency with classical theory exists. There is an increase in Nu with increasing Re measured. According to Herwig and Hausner [37], a common theoretical basis on forced convection for macro- and microchannels can be used to describe forced convection of liquids in the laminar regime. However, there are effects which are more pronounced and which are of more importance on the microscale, such as surface tension, viscous forces and electrostatic forces [38]. These effects are called "scaling effects" with respect to standard macroscale analysis.

There have been several approaches to identify these scaling effects of flow in microchannels, which lead to a discrepancy between classical theory and heat transfer in microchannels below 1 mm [39]. The deviations may be explained by general effects which are neglected in macroscale calculations but are of increasing importance as the characteristic size decreases.

A lower limit for hydraulic diameter of 1.2 mm was proposed by Adams *et al.* [23] for the applicability of standard turbulent single-phase Nusselt correlations.

In the following sections, the main deviations from classical theory for the calculation of heat transfer in microchannels are discussed. This discussion includes axial heat conduction in the fluid, conjugate heat transfer, surface roughness, viscous dissipation, thermophysical property variations, electric double layers, entrance region and measurement accuracy. Whenever possible, the reader is referred to design criteria and Nu correlations when the different aspects have to be taken into account.

9.4.1 Axial Heat Conduction in the Fluid

Axial conduction in the fluid leads to an increased temperature difference between the wall and the fluid. Therefore, Nu decreases in the entrance region. Axial

Table 9.1 *Nu* correlations for microchannels available in literature according to Figure 9.3 for $d_h \leq 1$ mm.

Ref.	d_h [μm]	Geometry	Material	Fluid	Range	Correlation
16	134–164	trap.	Si-glass	Nitrogen	$Re > 3000$ $163 < T < 298$	$Nu = 0.00222\ Re^{1.09} Pr^{0.4}$
17	9.7–81.2	circ.	Fused silica	Nitrogen	$Re < 2000$ $2500 < Re < 20000$ $293 < T < 333$	$Nu = 0.000972 Re^{1.17} Pr^{1/3}$ $Nu = 3.82 \times 10^{-6} Re^{1.96} Pr^{1/3}$
19	133–367	rect.	Stainless steel	Water	$50 < Re < 4000$ $295 < T < 317$	*laminar*: $Nu = C_{H,l} Re^{0.62} Pr^{1/3}$ *turbulent*: $Nu = C_{H,t} Re^{4/5} Pr^{1/3}$ $C_{H,l} = 0.0104$–0.0580, $C_{H,t} = 0.00483$–0.0926
18	310–747	rect.	Stainless steel	Methanol, DI water	$Re > 1000$–1500 $283 < T < 298$	$Nu = 0.00805\ Re^{4/5} Pr^{1/3}$
20	16.6–102	circ.	Fused silica	Nitrogen, DI water	$6000 < Re < 20000$	$Nu = 0.007\ Re^{1.2} Pr^{0.2}$
22	689	trap.	Si-glass	Water	$100 < Re < 4500$ $298 < T < 328$	*laminar*: $Nu = 8.39\ Re^{1/2}$–$1.33\ Re^{2/3}$ *turbulent*: $Nu = 4.73\ Re^{1/2}$–$0.22\ Re^{2/3}$
21	133–367	rect.	Stainless steel	Water	$50 < Re < 4000$	*laminar* : $Nu = 0.1165 \left(\frac{d_h}{W_c}\right)^{0.81} \left(\frac{H}{W}\right)^{-0.79} Re^{0.62} Pr^{1/3}$
					$293 < T < 318$	*turbulent* : $Nu = 0.072 \left(\frac{d_h}{W_c}\right)^{1.15} \left(1 - 2.421 \left(\frac{H}{W} - 0.5\right)^2\right) Re^{0.8} Pr^{1/3}$
33		circ.		Analytical, slip		$Nu = \frac{48(2\beta-1)^2}{(24\beta^2-16\beta+3)\left[1+\frac{24\kappa(\beta-1)(2\beta-1)^2}{(24\beta^2-16\beta+3)(\kappa+1)Pr}\right]}$ $\beta = 1 + 4Kn; \kappa = C_p/C_v$

34	$H = 100–580$, $W = 146–234$	rect.	Stainless steel	Oil, FC72	$70 < Re < 170$ (oil), $911 < Re < 4807$ (FC72)	$Nu_x = 0.429 Re^{0.583} Pr^{1/3} \left(\frac{x}{2H}\right)^{-0.394} \left(\frac{W}{2H}\right)^{-0.494}$
23	$760–1090$, $d_0 = 1164$	circ.	Copper	DI water	$2600 < Re < 23000$	$Nu = Nu_{Gn}\ (1 + F)$ $F = 7.6 \times 10^{-5} Re \left(1 - \left(\frac{d_h}{d_0}\right)^2\right)$
24	1131	non-circ.	Copper	Water	$3900 < Re < 21400$ $T = 323$	$Nu = Nu_{Gn}$
35	62–169	trap.	Si-glass	DI water	$100 < Re < 1400$	$Nu_{rough} = Nu_{theory} \left(\frac{Rm}{Rmw}\right)$
25	300	rect.	Copper	DI water	$600 < Re < 2800$	$Nu = 0.52 (RePrd_h/L)^{0.62}$ for $L/RePrd_h < 0.05$ $Nu = 2.02\ (RePrd_h/L)^{0.31}$ for $L/RePrd_h > 0.05$
26	$W = 158–1473$, $H = 56–111$	trap.	Si, SiO_2	DI water	$10 < Re < 1500$	$Nu = C_1 Re^{0.946} Pr^{0.488} \left(1 - \frac{c}{a}\right)^{3.547} \left(\frac{a}{H}\right)^{3.577} \times \left(\frac{\epsilon}{d_h}\right)^{0.041} \left(\frac{d_h}{L}\right)^{1.369}$ for $10 < Re < 100$ $Nu = C_2 Re^{0.148} Pr^{0.163} \left(1 - \frac{c}{a}\right)^{0.908} \left(\frac{a}{H}\right)^{1.001} \times \left(\frac{\epsilon}{d_h}\right)^{0.033} \left(\frac{d_h}{L}\right)^{0.798}$ for $100 < Re < 1500$
29	1800	circ.	Copper	Helium	$1600 < Re < 4000$ $110 < T < 250$	$Nu = 0.018 (Re_{inlet})^{0.805} (Pr_{inlet})^{0.41} + 14.25 Re_t^{-0.3879} \left(\frac{Pr_t}{Pr_{inlet}}\right)^{-226.6}$

(*Continued*)

Table 9.1 (*Continued*)

Ref.	d_h [μm]	Geometry	Material	Fluid	Range	Correlation
27	87	rect.	Si	Water	$20 < Re < 152$ $305 < T < 330$	$Nu = 4.1 + \frac{0.14(d_h/L)RePr}{1+0.05[(d_h/L)RePr]^{2/3}}$
28	531–1814	rect.	Brass, stainless steel	Nitrogen	$600 < Re < 5000$ $80 < T < 150$	$Nu = 55.15He^{0.948}\left(\frac{H}{W}\right)^{0.735}Re^{0.529}Pr^{1/3}$
30	1000	rect.	Stainless steel	Air, ethanol, methanol	$2297 < Re < 4275$ $347 < T < 390$	$Nu = 7.56\times10^{-7}Re^{1.38}Pr^{0.4}$
31		trap.		Numerical, no-slip	$0.1 < Re < 1000$	$Nu = \left[2.87\left(\frac{90^\circ}{\phi}\right)^{-0.26} + 4.8\,exp\left(-3.9\frac{H}{W}\left(\frac{90^\circ}{\phi}\right)^{0.21}\right)\right]G$ $G = \left[1+0.075\left(1+\frac{H}{W}\right)exp(-0.45Re)\right]$
32		trap.		Numerical, slip	$0.1 < Re < 10$	$Nu = \left[2.87\left(\frac{90^\circ}{\phi}\right)^{-0.26} + 4.8exp\left(-3.9\frac{H}{W}\left(\frac{90^\circ}{\phi}\right)^{0.21}\right)\right]G_2G_3$ $G_2 = \left[1+0.075\left(1+\frac{H}{W}\right)exp(-0.45Re)\right]$ $G_3 = 1-1.75Kn^{0.64}(1-0.72\tanh\left(2\frac{H}{W}\right)$
36			Si-glass	Analytical		$Nu = \frac{Nu_0}{1+\sigma Br}$ σ = geometry parameter

conduction does not affect a *Nu* at constant heat flux in fully developed flow [40]. At a constant wall temperature, axial conduction within the fluid can be neglected for $Pe > 10$ [41], where *Pe* is the Péclet number, $Pe = RePr$. Axial conduction in the fluid should be considered in the length x, where

$$\frac{x}{d_h} Pe \leq 20 \tag{9.11}$$

which is valid for the entrance region of a microchannel, for small *Re* and/or *Pr* [12]. This may be the case for liquid metals and gases at low *Re*. For most liquid applications, axial conduction within the fluid is insignificant and can be neglected.

9.4.2
Conjugate Heat Transfer

The contribution of the axial heat conduction in the channel walls to the total heat transfer depends on the ratio of the conductivities of the wall and the fluid, on the ratio of the wall thickness and channel diameter and on the Péclet number. As the wall thickness in macroscale applications is of small size compared with the channel diameter, axial conduction in the channel walls is neglected [41].

At low *Re* and when conjugate effects have to be considered, the temperature distribution along the microchannel is not linear. Under constant heat flux boundary conditions, *Nu* decreases with decreasing ratio of outer to inner channel diameter, approaching the constant temperature solution. A decrease in *Nu* is also seen with increasing wall conductivity. For constant temperature boundary conditions, *Nu* will increase approaching the constant heat flux solution with axial heat conduction in the wall. The values for local Nusselt number for the conjugated problem lie between the values for the two boundary conditions constant heat flux and constant temperature.

A criterion for the indication of axial heat transfer in the channel walls of heat exchangers has been proposed by Chiou [42], introducing a conduction parameter that represents the influence of axial heat conduction in the channel wall on the performance of the heat exchanger:

$$c = \frac{A_s/A_f}{L/d_h} \frac{1}{RePr} \frac{\lambda_s}{\lambda_f} \tag{9.12}$$

where A_s, A_f, λ_s and λ_f are the cross-sectional area and thermal conductivity for the channel wall (s) and the fluid (f), L is the channel length and d_h the hydraulic diameter. If the conductance number c is smaller than 0.005, the axial heat transfer through conduction in the channel wall can be neglected.

In microchannels, conjugate heat transfer leads to a complex three-dimensional heat flow pattern and Poiseuille flow may no longer be accurate [43]. Numerical simulations show that axial conduction in the channel wall does lower the Nusselt number but it is still in the range of conventional values [38]. The work of Gamrat *et al.* [44], in contrast, could not explain the lower Nusselt number by the axial conduction in the channel walls by numerical simulations.

Maranzana *et al.* [45] assumed a uniform heat transfer coefficient between a parallel plate microchannel. A dimensionless number M is introduced, which compares the conductive and convective heat flux in the walls and in the fluid, respectively:

$$M = \frac{r^2 NTU}{Bi} \tag{9.13}$$

where

$$NTU = \frac{hL}{\rho c_p d_f u} \tag{9.14}$$

$$Bi = \frac{h d_s}{\lambda_s} \tag{9.15}$$

r is the ratio of the wall thickness to the channel length, NTU the number of transfer units, h the convective heat transfer coefficient, L the channel length, d_f the channel height, u the mean fluid velocity, d_s the wall thickness and λs the wall conductivity. If M is smaller than 0.01, the axial conduction in the channel walls can be neglected.

Experimental and numerical studies of conjugated heat transfer at low *Re* were presented by Tiselj *et al.* [46]. A non-linear behavior of the temperature distribution was observed, caused by high values of axial heat flux in the channel wall. Nevertheless, the heat transfer is described by Navier–Stokes and energy equations.

If a conjugated problem has to be considered, the energy balance is extended to the whole fluid–solid system, in contrast to only fluid boundary conditions.

9.4.3
Surface Roughness

Roughness effects do not play an important role in laminar flow through pipes if the relative surface roughness is less than 5% [47]. The role of the surface roughness on *Nu* in microchannels in the laminar regime has not been explored thoroughly. However, the wall roughness influences the critical Reynolds number which defines the transition between laminar and turbulent flow. Qu *et al.* [35] observed significant differences between simulated and experimentally determined Nusselt numbers in trapezoidal microchannels with a relative surface roughness of 2.4–3.5%. They attributed the difference to surface roughness effects. The Nusselt number can be predicted by applying a roughness-viscosity model. As the roughness viscosity reduces the velocity gradient at the wall, the temperature gradient is also reduced, hence the convective heat transfer is lowered. This situation can be expressed by

$$Nu = Nu_{\text{theory}} \frac{\mu_{\text{Rm}}}{\mu_{\text{Rmw}}} \tag{9.16}$$

where Nu_{theory} is the theoretical Nusselt number from smooth microchannel and μ_{Rm} and μ_{Rmw} the average roughness viscosity over the cross-section and along the channel walls, respectively.

Wu and Cheng [26] derived a Nu correlation based on experimental results in trapezoidal Si microchannels. The surface roughness k is taken into account, in addition to geometric aspects:

$$Nu = C_1 Re^{0.946} Pr^{0.488} \left(1 - \frac{W_b}{W_t}\right)^{3.547} \left(\frac{W_t}{H}\right)^{3.577} \left(\frac{k}{d_h}\right)^{0.041} \left(\frac{d_h}{L}\right)^{1.369} \tag{9.17}$$

for $10 < Re < 100$, and $4.05 \leq Pr \leq 5.79$, $0 \leq W_b/W_t \leq 0.934$, $0.038 \leq H/W_t \leq 0.648$, $3.26 \times 10^{-4} \leq k/D_h \leq 1.09 \times 10^{-2}$ and $191.77 \leq L/D_h \leq 453.79$, and

$$Nu = C_2 Re^{0.148} Pr^{0.163} \left(1 - \frac{W_b}{W_t}\right)^{0.908} \left(\frac{W_t}{H}\right)^{1.001} \left(\frac{k}{d_h}\right)^{0.033} \left(\frac{d_h}{L}\right)^{0.798} \tag{9.18}$$

for $100 < Re < 1500$, and $4.44 \leq Pr \leq 6.05$, $0 \leq W_b/W_t \leq 0.934$, $0.038 \leq H/W_t \leq 0.648$, $3.26 \times 10^{-4} \leq k/D_h \leq 1.09 \times 10^{-2}$ and $191.77 \leq L/D_h \leq 453.79$, where $C_1 = 6.7$, $C_2 = 47.8$, W is the width of the channel at the bottom (b) and top (t), H is the channel height and L is the channel length.

Croce and D'Agaro [48] numerically investigated surface roughness effects on heat transfer in microtubes. In a plane channel, an increase in Nu with increasing surface roughness was reported, whereas Nu decreased in a circular tube with increasing roughness. The influence was dependent on the geometry of both the roughness elements and the channel and often in the range of experimental uncertainty.

9.4.4
Viscous Dissipation

The viscous dissipation is defined as mechanical energy which is irreversibly converted to thermal energy due to viscous effects in the fluid. The viscous dissipation is often taken into account by the Brinkman number, Br, which is the ratio of dissipation and heat diffusion:

$$Br = \frac{\mu u^2}{q_w} = \frac{\mu u^2}{\lambda \Delta T} = \frac{\mu^3 Re^2}{\rho^2 d_h^2 \lambda \Delta T} \tag{9.19}$$

where μ is the dynamic viscosity, u the average fluid velocity, q_w the heat flux at the wall, λ the thermal conductivity, ρ the fluid density and ΔT the representative temperature difference. The effect of viscous dissipation increases with decreasing channel size. In laminar flow, the viscous dissipation becomes important due to the large gradients in velocity and therefore large temperature gradients. With increasing Re, the importance of Br is reduced due to smaller gradients. In macroscale channels, the viscous dissipation can be neglected. Velocity gradients are too small in the laminar flow regime for the viscous dissipation to have a significant influence on the temperature in the fluid. An axial variation of Br due to viscosity changes influences the heat transfer in microchannels. Additionally, viscous dissipation is strongly dependent on the hydraulic diameter and the aspect ratio. From a dimension

analysis, Tso and Mahulikar [49] proposed a modified general form for Nu in the laminar regime in microchannels containing an empirical constant A' and a geometric function f depending on the critical microchannel dimension δ and the hydraulic diameter d_h:

$$Nu = A' Re^{0.62} Pr^{1/3} f(\delta, d_h) Br^d \tag{9.20}$$

The exponent d of Br is positive when the fluid in the microchannel is heated and negative when it is cooled.

Morini and Spiga [36, 50] demonstrated analytically the link between the average Nu and Br. A general relationship for circular and noncircular channels is

$$Nu = \frac{Nu_0}{1 + \sigma Br} \tag{9.21}$$

where Nu_0 is the value of Nu at $\mathrm{Br} = 0$ and σ is a parameter dependent on the channel geometry and the boundary conditions. Comparing the temperature increase by viscous dissipation and the increase by heat flux at the wall indicates the influence on the dissipation term in the energy balance. The ratio of the two contributions can be expressed by

$$\frac{\Delta\theta_v}{\Delta\theta_q} = 2Br \frac{A}{d_h^2} f\ Re \tag{9.22}$$

where A is the cross-sectional area of the microchannel and f the friction factor. To neglect the influence of viscous dissipation, the value of Equation (9.22) should not exceed 5%.

Koo and Kleinstreuer [51] showed for water that for channel sizes below 100 μm the viscous dissipation in the energy equation cannot be neglected.

9.4.5
Variation of Thermophysical Properties

At the microscale it is very important to take the variation of thermal properties of the fluid into consideration, especially at low Re [52].

The fluid viscosity and thermal conductivity experience the largest variation with temperature. Compared with the density and the specific heat variation, their influence on heat transfer is significantly higher, e.g. in the case of water. Therefore, density and thermal conductivity can in most cases be considered to be constant. The fluid property variation becomes more important with decreasing diameter, where the axial variation is more pronounced than the variation over the cross-section of the channel. In contrast to the viscous dissipation, the significance of property variations increases with decreasing Br [53].

Additionally, pressure-dependent properties in long microchannels have to be considered, since the pressure drop is significantly increased in small channels.

Morini [39] suggested that for gases constant properties can be assumed if the following conditions are fulfilled:

$$Ma = u/c < 0.2$$
$$\frac{\Delta p}{p_{\text{in}}} < 0.05 \tag{9.23}$$

where Ma is the average Mach number between the inlet and the outlet, u the average velocity of the fluid, c the acoustic velocity, Δp the pressure drop in the microchannel and p_{in} the initial static pressure.

For liquids and gases, it is proposed to adjust the properties of the fluid due to the temperature variations in the channel, where the viscosity of the liquid shows the most pronounced effect [40]:

$$\frac{Nu}{Nu_{\text{cp}}} = \left(\frac{\mu_{\text{w}}}{\mu_{\text{b}}}\right)^n \quad \text{for liquids}$$
$$\frac{Nu}{Nu_{\text{cp}}} = \left(\frac{T_{\text{w}}}{T_{\text{b}}}\right)^n \quad \text{for gases} \tag{9.24}$$

where cp denotes a constant property value and w and b indicate values at the wall and in the bulk, respectively. For liquids at laminar flow $n = -0.14$ and at turbulent flow $n = -0.11$ (heating) and $n = -0.25$ (cooling). For gases at laminar flow $n = 0$ and at turbulent flow $n = -0.5$ (heating) and $n = 0$ (cooling).

9.4.6
Electric Double Layer

Mala *et al.* [54] suggested that Nusselt numbers may be well overestimated if the effect of an electric double layer (EDL) at the fluid–solid interface in liquid flow is not considered. An EDL is formed when non-conducting channel materials are used. The layer modifies the velocity profile, which decreases the heat transfer. For channels sizes larger than 40 μm, the effect of the EDL can be neglected and therefore has no influence on the heat transfer [55].

9.4.7
Entrance Region

In general, the thermal entry region is described by the Hausen equation [Equation (9.33)]. For water flow in rectangular silicon microchannels, the coefficients of the Hausen equation were adapted by Li *et al.* [27]:

$$Nu = 4.1 + \frac{0.14(d_{\text{h}}/L)RePr}{1 + 0.05[(d_{\text{h}}/L)RePr]^{2/3}} \tag{9.25}$$

The thermal entry length l_{th} for laminar flow can be calculated by [40]

$$\frac{l_{th}}{d_h} = 0.05\, Re\, Pr \tag{9.26}$$

In turbulent flow, the entrance region is insignificant, since the turbulent thermal boundary layer develops very quickly.

Local Nusselt numbers were measured by Harms *et al.* [56] in deep silicon channels. The results agreed reasonably well with classical theory [41]. The small deviations were ascribed to the manifold geometry.

9.4.8
Measurement Accuracy

Standard temperature measurement in heat transfer experiments is still done using thermocouples. Thermocouple wires have diameters down to 12.7 μm. For shielded thermocouples, the smallest diameters available are in the region of 100 μm. The drawbacks are conduction losses through the thermocouple wire and flow disturbance. These errors are obviously more pronounced in microfluidic flows.

An example of an error analysis is shown in Equation (9.27). Usually *Nu* is calculated by measuring the temperature difference ΔT between the wall and the fluid and the heat input Q. The wall temperature is commonly measured by placing a thermocouple as close as possible to the wall and then applying simple heat conduction theory to estimate the actual temperature at the wall. The relative uncertainty of Nu, u_{Nu}/Nu, can be expressed by

$$\begin{aligned} Nu &= \frac{hd_h}{\lambda} = \frac{Qd_h}{A\Delta T\lambda} \\ \frac{u_{Nu}}{Nu} &= \left[\left(\frac{uQ}{Q}\right)^2 + \left(\frac{ud_h}{d_h}\right)^2 + \left(\frac{uA}{A}\right)^2 + \left(\frac{u\Delta T}{\Delta T}\right)^2 + \left(\frac{u\lambda}{\lambda}\right)^2\right]^{1/2} \end{aligned} \tag{9.27}$$

Qu *et al.* [35] reported an uncertainty of 8.5% for the *Nu* calculation and Tso and Mahulikar [57] stated a typical uncertainty of 9.2%. To estimate a correct value of Nu, the measurement of the geometric dimensions of the microchannel and the measurement of the wall temperature are very critical.

Non-intrusive temperature measurement techniques are liquid crystal thermometry [58], infrared thermometry and two color laser-induced fluorescence.

Thermal microscopy, reflectance thermometry and scanning optical thermometry measurement methods in micro- and nanodevices have been reviewed by Cahill *et al.* [59].

9.5
Conventional Heat Transfer Correlations for Macroscale Tubes and Channels

For the calculation of heat transfer coefficients in channels, conventional correlations in terms of macroscopic tubes and channels are listed in this section. For a critical

dimension for the validity of these correlations, a characteristic length of >1 mm is suggested [23, 39]. Nevertheless, a careful evaluation of the assumptions has to be carried out and, if necessary, adapted to include the above-discussed scaling effects.

9.5.1 Developing Hydrodynamic Regions of Laminar Flow

The hydrodynamic entry region l_h for laminar flow can be calculated by [60]

$$\frac{l_h}{d_h} = 0.05\,Re \tag{9.28}$$

9.5.2 Developing Thermal Flow

The thermal entry region for laminar flow can be calculated by [40]

$$\frac{l_{th}}{d_h} = 0.05\ Re\ Pr \tag{9.29}$$

9.5.3 Fully Developed Laminar Flow

We consider steady-state laminar and fully developed thermal and hydrodynamic single-phase flow.

9.5.3.1 Constant Wall Temperature

At constant wall temperature, the asymptotes from theory are predicted as follows:

$$Nu_{m,T,1} = 3.657 + 0.0499\ Re\ Pr\frac{d_i}{L} \tag{9.30}$$

for $Re\ Pr\ d_i/L \leq 33.3$ and

$$Nu_{m,T,2} = 1.615\left(RePr\frac{d_i}{L}\right)^{1/3} \tag{9.31}$$

for values of $Re\ Pr\ d_i/L > 33.3$.

For the whole range of $0 < Re\ Pr\ d_i/L < \infty$, the equation [61]

$$Nu_{m,T} = \left[Nu_{m,T,1}^3 + 0.7^3 + (Nu_{m,T,2} - 0.7)^3\right]^{1/3} \tag{9.32}$$

can be used.

With the Hausen correlation [13], Nusselt numbers in the thermal entry length can be calculated:

$$\overline{Nu} = 3.66 + \frac{0.0668(d_h/L)Re\ Pr}{1 + 0.04[(d_h/L)Re\ Pr]^{2/3}} \tag{9.33}$$

For a combined entry length, the Sieder–Tate [62] correlation is suitable:

$$\overline{Nu} = 1.86\left(\frac{Re\ Pr}{L/d_{\mathrm{h}}}\right)^{1/3}\left(\frac{u}{u_{\mathrm{w}}}\right)^{0.14} \tag{9.34}$$

for $Re < 2200$, $0.48 < Pr < 16\,700$ and $0.0044 < \mu/\mu_{\mathrm{w}} < 9.75$.

9.5.3.2 Constant Heat Flux

At constant heat flux, from theory the Nusselt numbers are predicted as follows [41]:

$$Nu_{m,H,1} = 4.36 + 0.0722 Re\ Pr \frac{d_{\mathrm{i}}}{L} \tag{9.35}$$

for $Re\ Pr\ d_{\mathrm{i}}/L < 33.3$ and

$$Nu_{m,H,2} = 1.953\left(Re\ Pr \frac{d_{\mathrm{i}}}{L}\right)^{1/3} \tag{9.36}$$

for $Re\ Pr\ d_{\mathrm{i}}/L \geq 33.3$.

For the whole range of $0 < Re\ Pr\ d_{\mathrm{i}}/L < \infty$, the equation [41]

$$Nu_{m,H} = [Nu_{m,H,1}^3 + 0.6^3 + (Nu_{m,H,2} - 0.6)^3]^{1/3} \tag{9.37}$$

can be used.

For asymptotic values of $Re\ Pr\ d_{\mathrm{i}}/L$, the mean Nu and friction factors are listed in Table 9.2, summarized from [41, 63], for constant wall temperature (T) and constant heat flux (H) at all four channel walls. Solutions for different boundary conditions can be found in [41].

9.5.4 Turbulent Flow

In turbulent flow, the boundary conditions "constant wall temperature" and "constant heat flux" lead to approximately the same mean Nusselt numbers. Correlations in the far turbulent regime ($Re > 10^4$) are noted here. The hydrodynamic entry length is approximately independent of Re, so that an approximation for fully turbulent flow after length x can be made for

$$\frac{x}{d_{\mathrm{h}}} > 10 \tag{9.38}$$

This expression can also be used for the thermal entrance region [40].

A widely used correlation in turbulent regime is the Dittus–Boelter correlation [15]:

$$Nu = 0.023 Re^{4/5} Pr^n \tag{9.39}$$

Table 9.2 Nusselt numbers and friction factors for different channel shapes in fully developed laminar flow.

Duct shape			Nu_H	Nu_T	$f\,Re$
Circular			4.364	3.657	16
Rectangular	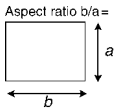	1	3.608	2.976	14.23
		2	4.123	3.391	15.55
		3	4.795	3.956	17.09
		4	5.331	4.439	18.23
		6	6.050	5.137	19.70
		8	6.490	5.597	20.58
		∞	8.235	7.541	24.00
Parallel plate			8.235	7.541	24.00
Hexagon			4.002	3.34	15.05
Isosceles triangle		10°	2.446	1.61	12.47
		30°	2.910	2.26	13.07
		60°	3.111	2.47	13.33
		70°	3.095	2.45	13.31
		90°	2.982	2.34	13.15
		120°	2.680	2.00	12.74
Ellipse	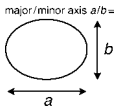	1	4.364	3.658	16.00
		1.5	4.438	–	16.31
		2	4.558	3.742	16.82
		4	4.880	3.792	18.24
		8	5.085	3.725	19.15
		16	5.176	3.647	19.54

with $n = 0.4$ for heating and $n = 0.3$ for cooling, for $0.7 < Pr < 160$, $Re > 10\,000$ and $L/D > 10$. This correlation is useful for small temperature changes. If larger temperature variations are expected, the correlation of Sieder and Tate [62] should be used:

$$Nu = 0.027 Re^{4/5} Pr^{1/3} \left(\frac{\mu}{\mu_w}\right) \tag{9.40}$$

for $0.7 < Pr < 16\,700$, $Re > 10\,000$ and $L/D > 10$.

9.5.4.1 Transition Regime $2300 < Re < 10^4$

A more complex but also more accurate correlation for the convective heat transfer in the transition regime is the Gnielinski correlation [14]:

$$Nu_{\mathrm{Gn}} = \frac{(f/8)(Re-1000)Pr}{1+12.7\sqrt{(f/8)}\left(Pr^{2/3}-1\right)}\left[1+\left(\frac{d}{L}\right)^{2/3}\right]\left(\frac{Pr}{Pr_{\mathrm{w}}}\right)^{0.11} \tag{9.41}$$

with the friction factor f from [64]:

$$f = (1.82\log Re - 1.64)^{-2} \tag{9.42}$$

The area of validity is $0.6 \leq Pr \leq 10^5$ and $2300 < Re < 10^6$.

The use of turbulent Nu correlations in the transition regime from laminar to turbulent flow must to be treated with caution. Heat transfer coefficient values will be overpredicted. An equation to calculate heat transfer rates in the transition region was proposed by Gnielinski [65]:

$$Nu = (1-\gamma)Nu_{l,2300} + \gamma Nu_{\mathrm{t},10^4} \tag{9.43}$$

$$\gamma = \frac{Re-2300}{10^4-2300},\ 0 \leq \gamma \leq 1 \tag{9.44}$$

where $Nu_{1,2300}$ and $Nu_{\mathrm{t},10^4}$ are the laminar and turbulent Nusselt numbers, respectively, at the corresponding Reynolds numbers from the Nu correlation for thermal and hydrodynamic entry regions.

The transition from laminar to turbulent flow in macroscale channels occurs at the critical Reynolds number of about $Re = 2300$. For flow in microchannels, an earlier transition to turbulent flow was indicated in earlier publications. However, recent studies show that in fluid flow at the microscale the critical Reynolds number is in the range of the macroscopic value.

The standard Nu correlations for different flow regimes are summarized in Table 9.3.

9.6 Conclusion

In this chapter, heat transfer from or to a fluid in microchannels with diameters of less than 1 mm was discussed. It was seen from the literature that correlations for Nusselt numbers in microchannels show little agreement whether heat transfer is enhanced or decreased at the microscale. The findings were often restricted to the individual setup used in a particular study. This leads to the conclusion that so far, no general correlation for heat transfer coefficients in microchannels can be suggested. The comparison with heat transfer analysis in macroscopic systems

Table 9.3 Summary of *Nu* correlations in conventional channels (>1 mm).

Ref.	Geometry	*Re* range	*Pr* range	Correlation	Comment
Laminar flow, fully developed flow					
41	circ.			$Nu = 3.6567935$	T
41	circ.			$Nu = 48/11 = 4.36364$	H
41	rect.			$Nu = 7.541(1 - 2.610\alpha^* + 4.970\alpha^{*2} - \mathrm{T},\ \alpha^* = H/W\ 5.119\alpha^{*3} + 2.702\alpha^{*4} - 0.548\alpha^{*5})$	T, $\alpha^* = H/W$
41	rect.			$Nu = 8.235(1 - 2.0421\alpha^* + 3.0853\alpha^{*2} - \mathrm{H},\ \alpha^* = H/W\ 2.4765\alpha^{*3} + 1.0578\alpha^{*4} - 0.1861\alpha^{*5})$	H, $\alpha^* = H/W$
Hydrodynamically developed flow, thermally developing flow					
41	circ.			$Nu = 3.657 + 0.0499\,RePr\frac{d_i}{L}$	T, $RePr\frac{d_i}{L} \leq 33.3$
66	circ.			$Nu = 1.615\left(RePr\frac{d_i}{L}\right)^{1/3}$	T, $RePr\frac{d_i}{L} > 33.3$
41	circ.			$Nu = 4.364 + 0.0722\,RePr\frac{d_i}{L}$	H, $RePr\frac{d_i}{L} < 33.3$
41	circ.			$Nu = 1.953\left(RePr\frac{d_i}{L}\right)^{1/3}$	H, $RePr\frac{d_i}{L} \geq 33.3$
13	circ.	$Re < 2200$	$\mathrm{Pr} \gg 1$	$Nu = 3.66\dfrac{0.0668(d_i/L)RePr}{1 + 0.04[(d_i/L)RePr]^{2/3}}$	T
Hydrodynamically and thermally developing flow					
62	circ.	$Re < 2200$	$0.48 < Pr < 16700$	$Nu = 1.86\left(\frac{RePr}{L/d_i}\right)^{1/3}\left(\frac{\mu}{\mu_w}\right)^{0.14}$	T, $0.0044 < \frac{\mu}{\mu_w} < 9.75$
Turbulent flow					
15	circ.	$Re > 10000$	$0.7 < Pr < 160$	$Nu = 0.023\,Re^{0.8}Pr^n$	$n = 0.4$ for heating,

(*Continued*)

Table 9.3 (*Continued*)

Ref.	Geometry	*Re* range	*Pr* range	Correlation	Comment
					$n = 0.3$ for cooling, $L/d_h > 10$
62	circ.	$Re > 10000$	$0.48 < Pr < 16700$	$Nu = 0.027 Re^{4/5} Pr^{1/3} \left(\frac{\mu}{\mu_w}\right)$	$L/d_h > 10$
Transition regime					
14		$2300 < Re < 10^6$	$0.6 < Pr < 10^5$	$Nu_{Gn} = \frac{(f/8)(Re-1000)Pr}{1+12.7\sqrt{(f/8)}(Pr^{2/3}-1)}\left[1+\left(\frac{d_h}{L}\right)^{2/3}\right]\left(\frac{Pr}{Pr_w}\right)^{0.11}$	$f = \frac{1}{(1.82\log_{10}(Re)-1.64)^2}$
65	circ.	$2300 < Re < 10000$		$Nu = (1-\gamma)Nu_{lam,2300}) + Nu_{turb,10^4}$	$\gamma = \frac{Re-2300}{10^4-2300}, 0 \leq \gamma \leq 1$

showed that several effects – which were neglected in larger systems – have to be considered at the microscale. These so-called "scaling effects" discussed in this chapter were axial heat conduction, surface roughness, viscous dissipation, thermophysical property variation, electric double layer and entrance region effects. The influence of scaling effects on heat transfer was explained, and criteria of applicability and recommendations for heat transfer calculations in microchannels were given.

List of Symbols and Abbreviations

Symbol	Units	Definition
A	m^2	Cross-sectional area
A'	–	Constant
n	–	number
k	$J\,K^{-1}$	Boltzmann constant
L, l	m	Length
u	$m\,s^{-1}$	Average fluid velocity
u		Uncertainty
m	kg	Mass
x, y, z	m	Coordinates
F	–	Factor
D, d	m	Diameter
r	–	Ratio
C	–	Constant
h	$W\,m^{-2}\,K^{-1}$	Convective heat transfer coefficient
M	–	Number
c_p	$J\,mol^{-1}\,K^{-1}$, $J\,kg^{-1}\,K^{-1}$	Specific heat capacity
W	m	Width
H	m	Height
k	m	Surface roughness
q	$W\,m^{-2}$, $W\,m^{-1}$	Heat flux
T	K	Temperature
f	–	Friction factor
c	$m\,s^{-1}$	Acoustic velocity
p	Pa	Pressure
Q	W	Heat
V	m^3	Volume
N_A	mol^{-1}	Avogadro's number

Greek Letters

λ	m	Mean free path
λ	$W\,m^{-1}\,K^{-1}$	Thermal conductivity

σ	m	Molecule diameter
σ	–	Parameter
δ_0	m	Mean molecular spacing
δ	m	Critical dimension
γ'	s^{-1}	Shear rate
τ	s	Molecular time scale
ε	J	Molecular energy scale
β	–	Factor
κ	–	Ratio of specific heats
ρ	$kg\,m^{-3}$	Density
μ	Pa s	Dynamic viscosity
θ	K	Temperature
Δ		Difference

Subscripts and Superscripts

IM	Intermolecular
Gn	Gnielinski
h	Hydraulic
0	Standard
s	Solid
f	Fluid
in	Initial
th	Thermal
w	Wall
b	Bottom
t	Top
ν	Viscous dissipation
q	Heat flux
b	Bulk
cp	Constant property
h	Hydrodynamic
m	Mean
T	Constant wall temperature
i	Inner
H	Constant heat flux
l	Laminar
t	Turbulent

Abbreviations

EDL	Electric double layer
NTU	Number of transfer units

References

1 D. B. Tuckerman, R. F. W. Pease, High-performance heat sinking for VLSI. *Electron Device Letters*, **1981**, *2*, 126–129.

2 S. G. Kandlikar, Fundamental issues related to flow boiling in minichannels and microchannels, *Experimental Thermal and Fluid Science*, **2002**, *26*, 389–407.

3 J. R. Thomé, Boiling in microchannels: a review of experiment and theory. *International Journal of Heat and Fluid Flow*, **2004**, *25*, 128–139.

4 M. Gad-el-Hak, The fluid mechanics of microdevices – The Freeman Scholar Lecture. *Journal of Fluids Engineering – Transactions of the ASME*, **1999**, *121*, 5–33.

5 G. A. Bird, *Molecular Gas Dynamics and the Direct Simulation of Gas Flows*, Clarendon Press, Oxford, **1994**.

6 C. Kleinstreuer, *Two-phase Flow Theory and Applications*, Taylor and Francis, New York, **2003**.

7 C. B. Sobhan, S. V. Garimella, A comparative analysis of studies on heat transfer and fluid flow in microchannels. *Microscale Thermophysical Engineering*, **2001**, *5*, 293–311.

8 A. A. Rostami, A. S. Mujumdar, N. Saniei, Flow and heat transfer for gas flowing in microchannels: a review. *Heat and Mass Transfer*, **2002**, *38*, 359–367.

9 B. Palm, Heat transfer in microchannels. *Microscale Thermophysical Engineering*, **2001**, *5*, 155–175.

10 N. T. Obot, Toward a better understanding of friction and heat/mass transfer in microchannels – a literature review. *Microscale Thermophysical Engineering*, **2002**, *6*, 155–173.

11 G. L. Morini, Single-phase convective heat transfer in microchannels: a review of experimental results. *International Journal of Thermal Sciences*, **2004**, *43*, 631–651.

12 G. Hetsroni, *et al.*, Heat transfer in microchannels: comparison of experiments with theory and numerical results. *International Journal of Heat and Mass Transfer*, **2005**, *48*, 5580–5601.

13 H. Hausen, *Verfahrenstechnische Zeitschrift VDI Beiheft*, **1943**, *8* (4), 91–98.

14 V. Gnielinski, New equations for heat and mass-transfer in turbulent pipe and channel flow. *International Chemical Engineering*, **1976**, *16*, 359–368.

15 F. W. Dittus, L. M. K. Boelter, Heat transfer in automobile radiators of the tubular type. *University of California Publications in Engineering*, **1930**, *2*, 443–461.

16 P. Wu, W. A. Little, Measurement of the heat-transfer characteristics of gas-flow in fine channel heat-exchangers used for microminiature refrigerators. *Cryogenics*, **1984**, *24*, 415–420.

17 S. B. Choi, R. F. Barron, R. O. Warrington, Fluid flow and heat transfer in microtubes, in *Micromechanical Sensors, Actuators and Systems*, **1991**, *ASME DSC-Volume 32*, p. 123–134.

18 B. X. Wang, X. F. Peng, Experimental investigation on liquid forced-convection heat-transfer through microchannels. *International Journal of Heat and Mass Transfer*, **1994**, *37*, 73–82.

19 X. F. Peng, G. P. Peterson, B. X. Wang, Heat transfer characteristics of water flowing through microchannels. *Experimental Heat Transfer*, **1994**, *7*, 265–283.

20 D. Yu, R. B. Warrington, T. Ameel, An experimental and theoretical investigation of fluid flow and heat transfer in microtubes, in *ASME/JSME Thermal Engineering Conference*, **1995**.

21 X. F. Peng, G. P. Peterson, Convective heat transfer and flow friction for water flow in microchannel structures. *International Journal of Heat and Mass Transfer*, **1996**, *39*, 2599–2608.

22 N. T. Nguyen, *et al.*, Investigation of forced convection in microfluid systems. *Sensors and Actuators A*, **1996**, *55*, 49–55.

23 T. M. Adams, *et al.*, An experimental investigation of single-phase forced convection in microchannels. *International Journal of Heat and Mass Transfer*, **1998**, *41*, 851–857.

24 T. M. Adams, *et al.*, Applicability of traditional turbulent single-phase forced convection correlations to non-circular microchannels. *International Journal of Heat and Mass Transfer*, **1999**, *42*, 4411–4415.

25 P. X. Jiang, *et al.*, Thermal-hydraulic performance of small scale micro-channel and porous-media heat-exchangers. *International Journal of Heat and Mass Transfer*, **2001**, *44*, 1039–1051.

26 H. Y. Wu, P. Cheng, An experimental study of convective heat transfer in silicon microchannels with different surface conditions. *International Journal of Heat and Mass Transfer*, **2003**, *46*, 2547–2556.

27 J. Li, G. P. Peterson, P. Cheng, Three-dimensional analysis of heat transfer in a micro-heat sink with single phase flow. *International Journal of Heat and Mass Transfer*, **2004**, *47*, 4215–4231.

28 H. L. Mo, *et al.*, Forced convection of low temperature nitrogen gas in rectangular channels with small aspect ratio. *Cryogenics*, **2004**, *44*, 301–307.

29 A. J. Jiao, S. Jeong, H. B. Ma, Heat transfer characteristics of cryogenic helium gas through a miniature tube with a large temperature difference. *Cryogenics*, **2004**, *44*, 859–866.

30 R. Rathnasamy, J. H. Arakeri, K. Srinivasan, Experimental investigation of forced convective heat transfer to air, liquids and liquid mixtures in a long narrow channel. *Proceedings of the Institution of Mechanical Engineers Part E – Journal of Process Mechanical Engineering*, **2005**, *219*, 311–317.

31 M. Renksizbulut, H. Niamand, Laminar flow and heat transfer in the entrance region of trapezoidal channels with constant wall temperature. *Journal of Heat Transfer – Transactions of the ASME*, **2006**, *128*, 63–74.

32 M. Renksizbulut, H. Niazmand, G. Tercan, Slip-flow and heat transfer in rectangular microchannels with constant wall temperature. *International Journal of Thermal Science*, **2006**, *45*, 870–881.

33 T. A. Ameel, *et al.*, Laminar forced convection in a circular tube with constant heat flux and slip flow. *Microscale Thermophysical Engineering*, **1997**, *1*, 303–320.

34 Y. Zhuang, C. F. Ma, M. Qin, Experimental study on local heat transfer with liquid impingement flow in two-dimensional micro-channels. *International Journal of Heat and Mass Transfer*, **1997**, *40*, 4055–4059.

35 W. L. Qu, G. M. Mala, D. Q. Li, Heat transfer for water flow in trapezoidal silicon microchannels. *International Journal of Heat and Mass Transfer*, **2000**, *43*, 3925–3936.

36 G. L. Morini, M. Spiga, The role of the viscous dissipation in heated microchannels. *Journal of Heat Transfer – Transactions of the ASME*, **2007**, *129*, 308–318.

37 H. Herwig, O. Hausner, Critical view on new results in micro-fluid mechanics: an example. *International Journal of Heat and Mass Transfer*, **2003**, *46*, 935–937.

38 Z. Y. Guo, Z. X. Li, Size effect on single-phase channel flow and heat transfer at microscale. *International Journal of Heat and Fluid Flow*, **2003**, *24*, 284–298.

39 G. L. Morini, Scaling effects for liquid flows in microchannels. *Heat Transfer Engineering*, **2006**, *27*, 64–73.

40 W. M. Kays, M. E. Crawford, B. Weigand, *Convective Heat and Mass Transfer*, 4th edn, McGraw-Hill Higher Education, Boston, MA, **2005**.

41 R. K. Shah, A. L. London, *Laminar Flow Forced Convection in Ducts: a Source Book for Compact Heat Exchanger Analytical Data*, Academic Press, New York, **1978**.

42 J. P. Chiou, The advancement of compact heat exchanger theory considering the effects of longitudinal heat conduction and flow nonuniformity, in *ASME Winter Annual Meeting, Compact Heat Exchangers: History, Technological Advancement and Mechanical Design Problems*, Chicago, **1980**.

43 A. G. Fedorov, R. Viskanta, Three-dimensional conjugate heat transfer in the microchannel heat sink for electronic packaging. *International Journal of Heat and Mass Transfer*, **2000**, *43*, 399–415.

44 G. Gamrat, M. Favre-Marinet, D. Asendrych, Conduction and entrance effects on laminar liquid flow and heat transfer in rectangular microchannels. *International Journal of Heat and Mass Transfer*, **2005**, *48*, 2943–2954.

45 G. Maranzana, I. Perry, D. Maillet, Mini- and micro-channels: influence of axial conduction in the walls. *International Journal of Heat and Mass Transfer*, **2004**, *47*, 3993–4004.

46 I. Tiselj, *et al.*, Effect of axial conduction on the heat transfer in micro-channels. *International Journal of Heat and Mass Transfer*, **2004**, *47*, 2551–2565.

47 L. F. Moody, N. J. Princeton, Friction factors for pipe flow. *Journal of Heat Transfer*, **1944**, *66*, 671–684.

48 G. Croce, P. D'Agaro, Numerical analysis of roughness effect on microtube heat transfer. *Superlattices and Microstructures*, **2004**, *35*, 601–616.

49 C. P. Tso, S. P. Mahulikar, The use of the Brinkman number for single phase forced convective heat transfer in microchannels. *International Journal of Heat and Mass Transfer*, **1998**, *41*, 1759–1769.

50 G. L. Morini, M. Spiga, Nusselt numbers in rectangular ducts with laminar viscous dissipation. *Journal of Heat Transfer – Transactions of the ASME*, **1999**, *121*, 1083–1087.

51 J. M. Koo, C. Kleinstreuer, Liquid flow in microchannels: experimental observations and computational analyses of microfluidics effects. *Journal of Micromechanics and Microengineering*, **2003**, *13*, 568–579.

52 M. Richter, P. Woias, D. Weiss, Microchannels for applications in liquid dosing and flow-rate measurement. *Sensors and Actuators A*, **1997**, *62*, 480–483.

53 S. P. Mahulikar, H. Herwig, Theoretical investigation of scaling effects from macro-to-microscale convection due to variations in incompressible fluid properties. *Applied Physics Letters*, **2005**, *86*, 014105.

54 G. M. Mala, D. Q. Li, J. D. Dale, Heat transfer and fluid flow in microchannels. *International Journal of Heat and Mass Transfer*, **1997**, *40*, 3079–3088.

55 C. Yang, D. Q. Li, J. H. Masliyah, Modeling forced liquid convection in rectangular microchannels with electrokinetic effects. *International Journal of Heat and Mass Transfer*, **1998**, *41*, 4229–4249.

56 T. M. Harms, M. J. Kazmierczak, F. M. Gerner, Developing convective heat transfer in deep rectangular microchannels. *International Journal of Heat and Fluid Flow*, **1999**, *20*, 149–157.

57 C. P. Tso, S. P. Mahulikar, Experimental verification of the role of Brinkman number in microchannels using local parameters. *International Journal of Heat and Mass Transfer*, **2000**, *43*, 1837–1849.

58 A. Gunther, P.R. von Rohr, Structure of the temperature field in a flow over heated waves. *Experiments in Fluids*, **2002**, *33*, 920–930.

59 D. G. Cahill, K. Goodson, A. Majumdar, Thermometry and thermal transport in micro/nanoscale solid-state devices and structures. *Journal of Heat Transfer – Transactions of the ASME*, **2002**, *124*, 223–241.

60 H. L. Langhaar, Steady flow in the transition length of a straight pipe. *Journal of Applied Mechanics*, **1942**, *64*, A55–A58.

61 V. Gnielinski, Heat-transfer on laminar-flow in tubes and constant wall temperature. *Chemie Ingenieur Technik*, **1989**, *61*, 160–161.

62 E. N. Sieder, G. E. Tate, Heat transfer and pressure drop of liquids in tubes. *Industrial and Engineering Chemistry*, **1936**, *28*, 1429–1435.

63 S. Kakaç, *Handbook of Single-phase Convective Heat Transfer*, John Wiley & Sons, Inc., New York, **1987**.

64 G. K. Filonenko, Hydraulic resistance in pipes. *Teploenergetika*, **1954**, *4*, 40–44.

65 V. Gnielinski, New method to calculate heat-transfer in the transition region between laminar and turbulent tube flow. *Forschung im Ingenieurwesen – Engineering Research*, **1995**, *61*, 240.

66 VDI, *VDI-Wärmeatlas*, Springer, Berlin, **2006**.